Title
EFFECTIVE ATMOSPHERIC LOSSES FOR 125-MeV PROTONS IN SOUTH ATLANTIC ANOMALY

Authors
Heckman, Harry H.
Brady, Victor O.

Publication Date
1965-12-23

UCRL-16592

University of California
Ernest O. Lawrence Radiation Laboratory

EFFECTIVE ATMOSPHERIC LOSSES FOR 125-MeV PROTONS IN SOUTH ATLANTIC ANOMALY

Berkeley, California

DISCLAIMER

Submitted to Journal of
Geophysical Research

UCRL-16592

UNIVERSITY OF CALIFORNIA

Lawrence Radiation Laboratory
Berkeley, California

Contract No. W-7405-eng-48

EFFECTIVE ATMOSPHERIC LOSSES FOR 125-MeV PROTONS IN SOUTH ATLANTIC ANOMALY

Harry H. Heckman and Victor O. Brady

December 23, 1965

EFFECTIVE ATMOSPHERIC LOSSES FOR 125-MeV PROTONS IN SOUTH ATLANTIC ANOMALY

Harry H. Heckman and Victor O. Brady

Lawrence Radiation Laboratory
University of California
Berkeley, California
December 23, 1965

ABSTRACT

Orbit calculations are carried out to evaluate the effective atmospheric densities for geomagnetically trapped 125-MeV protons whose guiding centers mirror between 200- and 560-km altitude in the South Atlantic anomaly. Such orbits are limited to the region of B-L space $L = 1.38$ and $0.2043 < B_m < 0.2355$ gauss. Calculated are the effective atmospheric densities and scale heights experienced by the particle and its guiding center. Rates of energy loss by ionization are also calculated, taking into account atmospheric composition and the ionization energies for each constituent. Atmospheres used in the computations are the Harris and Priester S = 100 and S = 200 models, each diurnally averaged, and the Johnson model for solar minimum. The geomagnetic field is described by the 48-term spherical harmonic expansion of Jensen and Cain.

INTRODUCTION

Relevant to problems that involve particle-loss rates to the atmosphere is the evaluation of the effective atmospheric density traversed by geomagnetically trapped particles. In order to limit computation time, it is customary to invoke the assumption that particle motion is completely described by the leading terms in the asymptotic series for the adiabatically invariant magnetic moment, $\mu = (mv_\perp^2/2B) + \ldots$, and the longitudinal adiabatic invariant, $J = \oint p_{||}\, ds + \ldots$. [Northrop, 1963]. The calculations of Newkirk and Walt [1964], Blanchard and Hess [1964], Cornwall, Sims and White [1965], and Hassitt [1965] were carried out according to this procedure. The effective atmospheric densities that have been calculated pertain, therefore, to an average along the particle's guiding-center motion, rather than to the actual trajectory of the particle. For low-rigidity particles, the guiding-center approximation is certainly valid for atmosphere averaging. For energetic protons, $E \gtrsim 100$ MeV, however, the gyroradii become comparable to the scale-height of the atmosphere at low altitudes and, as a result, the atmospheric densities encountered by the particle may differ appreciably from those encountered by its guiding center.

The need for a more accurate calculation of effective atmospheric densities traversed by low-altitude mirroring protons stems from the experiments of Heckman and Nakano [1965]. By measuring the east-west asymmetries in the flux of mirroring protons, $E > 100$ MeV, in the region of the South Atlantic anomaly, Heckman and Nakano have determined mirror-point density scale-heights as a function of minimum mirror-point altitudes between 300 and 450 km. The confidence with which

(1962).]

If, in vector notation, $\underset{\sim}{Y}'(s) = \underset{\sim}{F}[s,\underset{\sim}{Y}(s)]$ is a system of first-order ordinary differential equations for which the solution is known at four points s, s-δ, s-2δ, s-3δ for some step size δ, then the Adam's method consists of using the formula

$$\underset{\sim}{Y}(s + \delta) = \underset{\sim}{Y}(s) + \delta \frac{[55\underset{\sim}{Y}'(s) - 59\underset{\sim}{Y}'(s - \delta) + 37\underset{\sim}{Y}'(s - 2\delta) - 9\underset{\sim}{Y}'(s - 3\delta)]}{24}$$

for predicting the solution at s + δ, and the formulas

$$\underset{\sim}{Y}'(s + \delta) = \underset{\sim}{F}[s + \delta, \underset{\sim}{Y}(s + \delta)]$$

$$\underset{\sim}{Y}(s + \delta) = \underset{\sim}{Y}(s) + \delta \frac{[9\underset{\sim}{Y}'(s + \delta) + 19\underset{\sim}{Y}'(s) - 5\underset{\sim}{Y}'(s - \delta) + \underset{\sim}{Y}'(s - 2\delta)]}{24}$$

for improving the predicted value. A corrected value of $\underset{\sim}{Y}'(s + \delta)$ is then computed from the new value of $\underset{\sim}{Y}(s + \delta)$.

The four needed starting values are obtained by four applications of the Runge-Kutta method. If the solution is known at a point s, then the Runge-Kutta method consists of use of the formula

$$\underset{\sim}{Y}(s + \delta) = \underset{\sim}{Y}(s) + \delta \frac{(\underset{\sim}{A} + 2\underset{\sim}{B} + 2\underset{\sim}{C} + \underset{\sim}{D})}{6}$$

where

$$\underset{\sim}{A} = \underset{\sim}{F}[s,\underset{\sim}{Y}(s)]$$

$$\underset{\sim}{B} = \underset{\sim}{F}[s + \delta/2, \underset{\sim}{Y}(s) + \delta\underset{\sim}{A}/2]$$

$$\underset{\sim}{C} = \underset{\sim}{F}[s + \delta/2, \underset{\sim}{Y}(s) + \delta\underset{\sim}{B}/2]$$

$$\underset{\sim}{D} = \underset{\sim}{F}[s + \delta, \underset{\sim}{Y}(s) + \delta\underset{\sim}{C}].$$

In order to determine the proper value for the step size δ, the equations were solved with a dipole field used as an approximation to the earth's magnetic field. The amount that the unit velocity $d\ell/ds = (x^2 + y^2 + z^2)^{\frac{1}{2}}$ deviates from one was taken as a measure of the

computational error. Although some programs for computing charged-particle orbits use a variable step size [McCracken, Rao, and Shea, 1962], our calculations with the dipole field showed no advantageous reason to do so. We therefore chose, on the basis of these calculations, a fixed step size of 5 kilometers of arc length. In the calculations involving a model of the earth's actual field, the maximum relative error of the magnitude of $d\ell/ds$ was found to be about 0.05 per cent.

Guiding-center coordinates. Concurrent with the step-wise integration of the equations of motion, we performed an additional calculation at selected points along the particle orbit to determine the polar coordinates of the instantaneous guiding center of the particle orbit. We define the vector coordinate of the guiding center, $\underset{\sim}{r}'$, by the equation $\underset{\sim}{r}' = \underset{\sim}{r} + \underset{\sim}{\rho}$. The position of the particle is denoted by the vector $\underset{\sim}{r}$ and the gyroradius vector $\underset{\sim}{\rho} = (B\rho/B^2)[\hat{v} \times \underset{\sim}{B}]$, Fig. 1.

EFFECTIVE ATMOSPHERIC LOSSES AND SCALE HEIGHTS

Model atmospheres. In our calculations we have used two diurnally averaged model atmospheres of Harris and Priester (H and P)[1962] appropriate for times near solar maximum (S = 200) and solar minimum (S = 100), and the low-density, solar-minimum atmosphere given by Johnson [1965]. Because the concentration-vs-altitude relationships for the constituents N_2, O_2, O, He, and H of these model atmospheres are approximately exponential, they were fitted, for computational purposes, by the method of least squares to a polynomial of the form

$$\ell n \left[C_i (R) \right] = \sum_{k=1}^{4} H_{ik} R^{k-1}, \qquad (3)$$

where R denotes altitude (km) and $C_i(R)$ concentration (number/cm^3)

for the ith constituent. The least-squares coefficients, H_{ik}, for each constituent of the H and P and Johnson model atmospheres for altitudes above 150 km are listed in Table 1. Because trapped particles on magnetic shell L = 1.4 attain altitudes up to 3500 km, it was necessary to extrapolate the fitted He and H concentration curves above the maximum altitudes listed by Harris and Priester (2050 km) and Johnson (2500 km). The extrapolated He and H curves exhibit proper functional behavior, and are, therefore, sufficiently realistic for atmospheric calculations -- particularly when one notes the present uncertainties in the hydrogen densities at these altitudes [Cornwall et al., 1965]. Whereas the H and P model gives a hydrogen concentration that is less at solar minimum than at solar maximum, the Johnson model, as well as that of Anderson and Francis [1965], indicates that the concentration is greater at minimum. On the basis of the H and P model, hydrogen concentrations at solar minimum can be predicted that differ by nearly an order of magnitude from that based on the Johnson solar-minimum-atmospheric model (Fig. 2). For this reason we have chosen these two models for computation and comparison. At solar maximum there are no significant differences among the model atmospheres, and we have taken the time-averaged H and P S=200 atmosphere as representative for this period of the solar cycle.

Atmospheric density and stopping power. The density and stopping power of the atmosphere were computed by a subroutine called AIR, which was given the proton's kinetic energy T, altitude R, and coefficients H_{ik}.

$$\rho(R) = 1.660 \times 10^{-24} \sum_i A_i \, C_i \, (R) \quad g/cm^3 \qquad (4)$$

$$\frac{dT}{ds}(R) = 1.660 \times 10^{-24} \sum_i (dT/ds)_i \, A_i C_i(R) \quad MeV/cm. \qquad (5)$$

The formula for the stopping power for element i, $(dT/ds)_i$, expressed in MeV $g^{-1}cm^2$, was obtained by differentiating the range-energy relation given by Barkas and Berger [1964]. The ionization energies, I, that were used to evaluate $(dT/ds)_i$ are: nitrogen, 88 eV; oxygen, 101 eV; He, 42 eV; and $H_{(atomic)}$, 15 eV [Fano, 1963].

Specified by the initial conditions for the orbit calculations were the particle's kinetic energy, altitude, co-latitude, and longitude at its minimum mirror-point altitude. The atmospheric density and stopping power were calculated at 40-km intervals along the particle's trajectory. The atmospheric density was also calculated for the orbit's guiding-center altitude at these same points. The following quantities were evaluated:

a) the amount of atmosphere traversed by the particle between the jth and $(j + 1)$th conjugate mirror points,

$$\int_j^{j+1} \rho(R) \, ds \quad (g/cm^2) \quad \text{and}$$

b) the resultant energy loss,

$$\int_j^{j+1} \frac{dT}{ds}(R) \, ds \quad (MeV),$$

c) the atmosphere traversed by the particle when the atmospheric density is equal to that at its guiding center,

$$\int_j^{j+1} \rho(R')\, ds \ (g/cm^2),$$

d) the integrated path length

$$\int_j^{j+1} ds, \quad \text{and}$$

e) the mirror-point coordinates of the guiding center, R', θ', ϕ', and magnetic-field value $B(R')$.

Upon completion of the integrations, quantities a) through d) were summed over j, the number of mirror points.

When the initial conditions of the orbit were chosen to be the point of maximum atmospheric density, the atmosphere traversed per bounce diminished rapidly as the particle drifted away from its starting point in the South Atlantic anomaly. Thus as the integration proceeded, the atmosphere traversed by the particle on the jth bounce was examined, and if

$$\rho_j \Big/ \sum_{j=1}^{j} \rho_j \leq 4 \times 10^{-4},$$

the integration was ended. This criterion allowed a maximum of 1% error in the integrated atmospheric densities, and significantly decreased computation time. The computation was completed by returning to the initial point and integrating the equations of motion in negative time.

RESULTS AND DISCUSSION

Figure 3(a) is a representative mirror-point trajectory obtained from the equations of motion of a 125-MeV proton ($\beta = 0.470$) where

$B_m(R') = 0.209$ gauss and $L = 1.38$. Plotted are the (160) consecutive mirror-point coordinates, R' vs ϕ', of the guiding-center trajectory during one drift period. The longitudinal drift velocities of the guiding center in the north and south hemispheres are given in Fig. 3(b). Here, $\dot{\phi}'$ equals $\Delta\phi'/\Delta t(\phi')$, where $\Delta\phi'$ is the change in longitude between successive mirror points in the respective hemispheres, and $\Delta t(\phi')$ is the bounce period. As first demonstrated by Newkirk and Walt [1964], guiding-center drift velocities of radiation trapped in the earth's nondipolar magnetic field can vary as much as 30% from the mean at $B_m = 0.237$, $L = 1.25$. For the particular trajectory illustrated in Fig. 3, we find $\dot{\phi}'_{max}/\dot{\phi}_{mean} = 1.41$, with a maximum variation of $\dot{\phi}'_{max}/\dot{\phi}'_{min} = 1.65$. The minimum and maximum values of the angular drift velocity occur near -55° longitude in the northern and southern hemispheres, respectively. The length of the longitudinal drift period -- 17.5 seconds -- gives a mean angular drift velocity of 0.357 rad/sec.

The results of our calculations on the atmosphere traversed, in units g/cm^2 per drift period, are presented in Fig. 4. For each of the three atmospheric models are shown (a) the atmosphere traversed by the particle, $\rho(R)$, and (b) the atmosphere traversed by the particle's guiding center $\rho(R')$ between minimum guiding-center altitudes 200 and 560 km. For each model atmosphere, curves of the resultant energy loss by ionization per drift period versus altitude are given in Fig. 5. The effect of finite gyroradii on the calculated densities, Fig. 4, are most evident at the lowest altitudes, where a 125-MeV proton encounters approximately twice the density of atmosphere per drift period

as does its guiding center. Above 250 kilometers, however, the differences between the effective atmospheres encountered by a particle and its guiding center are clearly less important than those due to solar-cycle changes in the composition and density of the atmosphere.

The final results of these calculations are given in Fig. 6, where the altitude dependence of the density scale height, h, of each model atmosphere is compared with (a) h_ρ, the density scale height averaged over the particle's trajectory; (b) $h_{\Delta E}$, the energy-loss scale height; and (c) $h_{\rho'}$, the density scale height averaged over the guiding-center trajectory. The scale height, or e-folding distance, h, for the atmospheric density ρ is calculated from the expression $h = -\Delta R/\Delta \ell n\rho$, where $\Delta \ell n\rho$ is the change in $\ell n\rho$ over the increment in altitude ΔR. The scale heights, h_ρ, $h_{\Delta E}$ and $h_{\rho'}$ are similarly defined, where $\Delta R = R_2' - R_1'$ is the increment in the minimum guiding-center altitude. Plotted against the scale height in Fig. 6 is the mean guiding-center altitude, $\frac{1}{2}(R_1' + R_2')$.

The altitude dependence of the various calculated scale-height quantities for each model atmosphere is qualitatively the same. At the lowest altitudes, where the important constituents of the atmosphere are N_2, O_2, and O ($A/Z = 2$) and the rate of energy loss is proportional to the atmospheric density, $h_{\Delta E}$ is equal to h_ρ. Above 300 km, the presence of the helium and hydrogen components becomes increasingly evident. Owing to changes in the average A/Z ratio and the (increased) stopping power of the atmosphere, the ionization energy losses no longer are proportional to atmospheric density. As a consequence, $h_{\Delta E}$ is greater than h_ρ at the higher altitudes.

Differences in the effective atmospheres averaged over the particle and guiding-center orbits are manifest in the differences between h_ρ and $h_{\rho'}$. Because a particle always penetrates the densest portion of atmosphere below its guiding center, it traverses (on the average) an atmosphere that has a scale height less than that traversed by the guiding center. Hence, h_ρ is less than $h_{\rho'}$ at all altitudes.

In order to determine the sensitivity of the effective scale-height curves (Fig. 6) to changes in the concentration of hydrogen, we arbitrarily increased the hydrogen concentration in the H and P S = 100 atmosphere 2.5 times. We find that the resultant effective scale-heights calculated from this modified atmospheric model are increased by only 0.75 to 1.4% (maximum) over those calculated with the unmodified atmospheric model.

SUMMARY

The possibility for interpreting low-altitude radiation measurements in the region of the South Atlantic anomaly in terms of atmospheric losses and their solar-cycle variations has led us to examine in detail the effects of particle motion in the earth's magnetic field on the average atmospheric densities and scale-heights encountered by the particle and its guiding center. The calculations are specific for 125-MeV protons that mirror on the magnetic-shell parameter $L = 1.38$, and $0.2043 < B_m < 0.2355$ gauss, a region geographically centered in the anomaly, at 200- to 560-km altitude. The numerical results, which have relevance to trapped particles whose gyroradii are comparable to the density scale-heights of the atmosphere, show that for 125-MeV protons:

a) The effective atmospheric density averaged over the particle's motion is about twice the density averaged over the guiding-center's trajectory.

b) The scale-heights, h_ρ and $h_{\rho'}$, evaluated from the above-averaged atmospheric densities, can be 3 to 4 times the vertical density scale-height h of the model atmosphere, the number depending on altitude and time in solar cycle -- in agreement with the results of Newkirk and Walt, [1964].

c) The changes in atmospheric composition with increasing altitude cause the ratio $h_{\Delta E}/h_\rho$ to change from 1 (at low altitudes where $\Delta E \propto \rho$) to 1.6 (owing to the increased stopping power of the He and H constituents), the actual number again depending on altitude and time in the solar cycle. Because of the averaging effects of particle motion, the effective scale heights $h_{\rho'}$, h_ρ, and $h_{\Delta E}$ increasingly diverge from h, the vertical density scale-height above 400 to 500 km.

Acknowledgments. We thank Dr. Donald V. Reames for his assistance in formulating and programming the subroutine AIR used in these calculations. This work was performed under the auspices of the U. S. Atomic Energy Commission, Contract No. 7405-eng-48.

TABLE 1. Least Squares Coefficients H_{ik} (Eq. 3)
for Altitudes > 150 km

Model	Constituent				
	N_2	O_2	O	He	H
	2.869E 01*	2.742E 01	2.473E 01	1.590E 01	9.34E 00
H and P S=200	-3.559E-02	-4.023E-02	-1.554E-02	-3.761E-03	-8.813E-04
T_{av} = 1441° K	2.578E-05	2.933E-05	4.876E-06	8.486E-07	1.449E-07
	-1.113E-08	-1.275E-08	-9.273E-10	-1.263E-10	-1.578E-11
	3.210E 01	3.127E 01	2.682E 01	1.659E 01	9.915E 00
H and P S=100	-6.210E-02	-7.070E-02	-2.766E-02	-5.796E-03	-1.428E-03
T_{av} = 869° K	6.188E-05	7.165E-05	1.308E-05	1.139E-06	2.240E-07
	-3.724E-08	-4.366E-08	-4.120E-08	-1.371E-10	-2.207E-11
Johnson	3.081E 01	3.006E 01	2.709E 01	1.590E 01	1.370E 01
solar	-5.114E-02	-6.072E-02	-2.951E-02	-6.412E-03	-1.941E-03
minimum	1.149E-05	1.698E-05	6.698E-06	1.067E-06	4.288E-07
T = 700° K	-1.898E-09	-3.364E-09	01.098E-09	-1.793E-10	-7.002E-11
T_H = 930° K					

* 2.869E 01 = 2.869×10^1

References

Anderson, A. D., and W. E. Francis, Tables of neutral atmospheric properties as a function of solar activity and local time from 90 to 10 000 km. Lockheed Report, 6-75-65-19, 1965.

Barkas, W. H., and M. J. Berger, Tables of energy losses and ranges of heavy charged particles, NAC-NRC Publication 1133, Nuclear Science Series Report 39, 103, 1964.

Blanchard, R. C., and W. N. Hess, Solar cycle changes in inner-zone protons, J. Geophys. Res, 69, 3927-3938, 1964.

Cornwall, J. M., A. R. Sims, and R. S. White, Atmospheric density experienced by radiation belt protons, J. Geophys. Res., 70, 3099-3116, 1965.

Dragt, A. J., Trapped orbits in a magnetic dipole, Rev. Geophys. 3, 255-298, 1964.

Fano, U., Penetration of Protons, alpha particles and mesons, Ann. Rev. of Nuclear Sci., 13, 1, 1963.

Freden, S. C., and G. A. Paulikas, Trapped protons at low altitudes in the South Atlantic anomaly, J. Geophys. Res., 69, 1259-1269, 1964.

Harris, I., and W. Priester, Theoretical models for the solar-cycle variation of the upper atmosphere, Goddard Space Flight Center, National Aeronautics and Space Administration, Rept. X-640-62-70, 1962.

Hassitt, A., Average effect of the atmosphere on trapped protons, J. Geophys. Res., 70, 5385-5394, 1965.

Heckman, H. H., and G. H. Nakano, Direct observations of mirroring protons in the South Atlantic anomaly, in Space Research V,

edited by D. G. King-Hele et al., North Holland Publishing Company, Amsterdam, 329-342, 1965.

Henrici, P., Discreet Variable Methods in Ordinary Differential Equations, John Wiley and Sons, New York, 1962.

Jensen, D. C., and J. C. Cain, An interim magnetic field, J. Geophys. Res., 67, 3568, 1962.

Johnson, F. S., Structure of the upper atmosphere, in Satellite Environment Handbook, Second Edition, edited by F. S. Johnson, 3-20, Stanford University Press, Stanford, California 1965.

McCracken, K. G., U. R. Rao, and M. A. Shea, The trajectories of cosmic rays in a high degree simulation of the geomagnetic field, Mass. Inst. Tech. Tech Rept. 77, August 1962.

Newkirk, L. L., and M. Walt, Longitudinal drift velocity of geomagnetically trapped particles, J. Geophys. Res., 69, 1759-1763, 1964.

Northrop, T. G., The Adiabatic Motion of Charged Particles, Interscience Publishers, New York, 1963.

Figure Captions

Fig. 1. Particle and guiding-center coordinates in earth-centered, spherical polar-coordinate system.

Fig. 2. (a) Diurnally averaged Harris and Priester model atmosphere for S = 100 (10^{-22} W m^{-2} cps^{-1}).

(b) Johnson solar-minimum atmosphere. Curves are least-squares fits to the tabular data for each constituent. Representative data points from each model are shown.

Fig. 3. (a) Guiding-center mirror-point trajectories in the northern and southern hemispheres for 125-MeV proton (β = 0.470), B_m = 0.209, and L = 1.38. Several sets of conjugate mirror points are identified by larger circles.

(b) Longitudinal angular-drift velocities of the guiding-center for the mirror-point trajectories shown in Fig. 3(a).

Fig. 4. Calculated "thickness" of atmospheres (g/cm^2) traversed per drift period by a proton (β = 0.470) and its guiding center as a function of the minimum guiding-center altitude. L = 1.38.

Fig. 5. Calculated rates of energy loss by ionization versus altitude of minimum guiding-center altitude for the model atmospheres of Harris and Priester and of Johnson.

Fig. 6. Atmospheric density and effective scale heights versus altitude for the diurnally averaged Harris and Priester S = 200 and S = 100 atmospheres, and the Johnson solar-minimum atmosphere. The density scale-height curve for each model atmosphere is labeled h; h_ρ is the density scale height averaged over the particle's trajectory; $h_{\Delta E}$ is the energy-loss scale height;

and $h_{\rho'}$ is the density scale height averaged over the guiding-center trajectory.

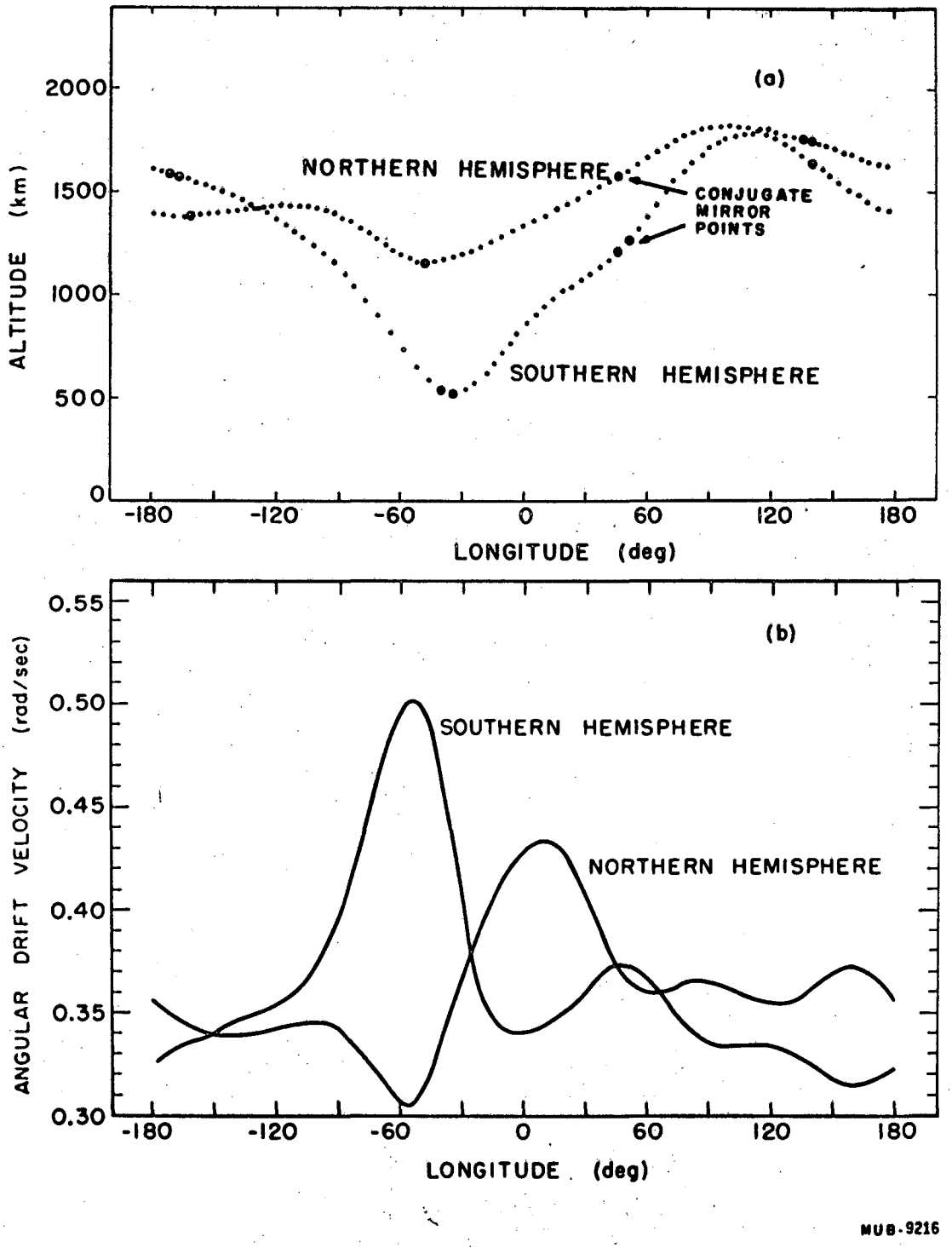
(a)
NORTHERN HEMISPHERE
CONJUGATE MIRROR POINTS
SOUTHERN HEMISPHERE
ALTITUDE (km)
2000
1500
1000
500
0
-180
-120
-60
0
60
120
180
LONGITUDE (deg)
(b)
SOUTHERN HEMISPHERE
NORTHERN HEMISPHERE
ANGULAR DRIFT VELOCITY (rad/sec)
0.55
0.50
0.45
0.40
0.35
0.30
LONGITUDE (deg)
MUB-9216

Fig. 3

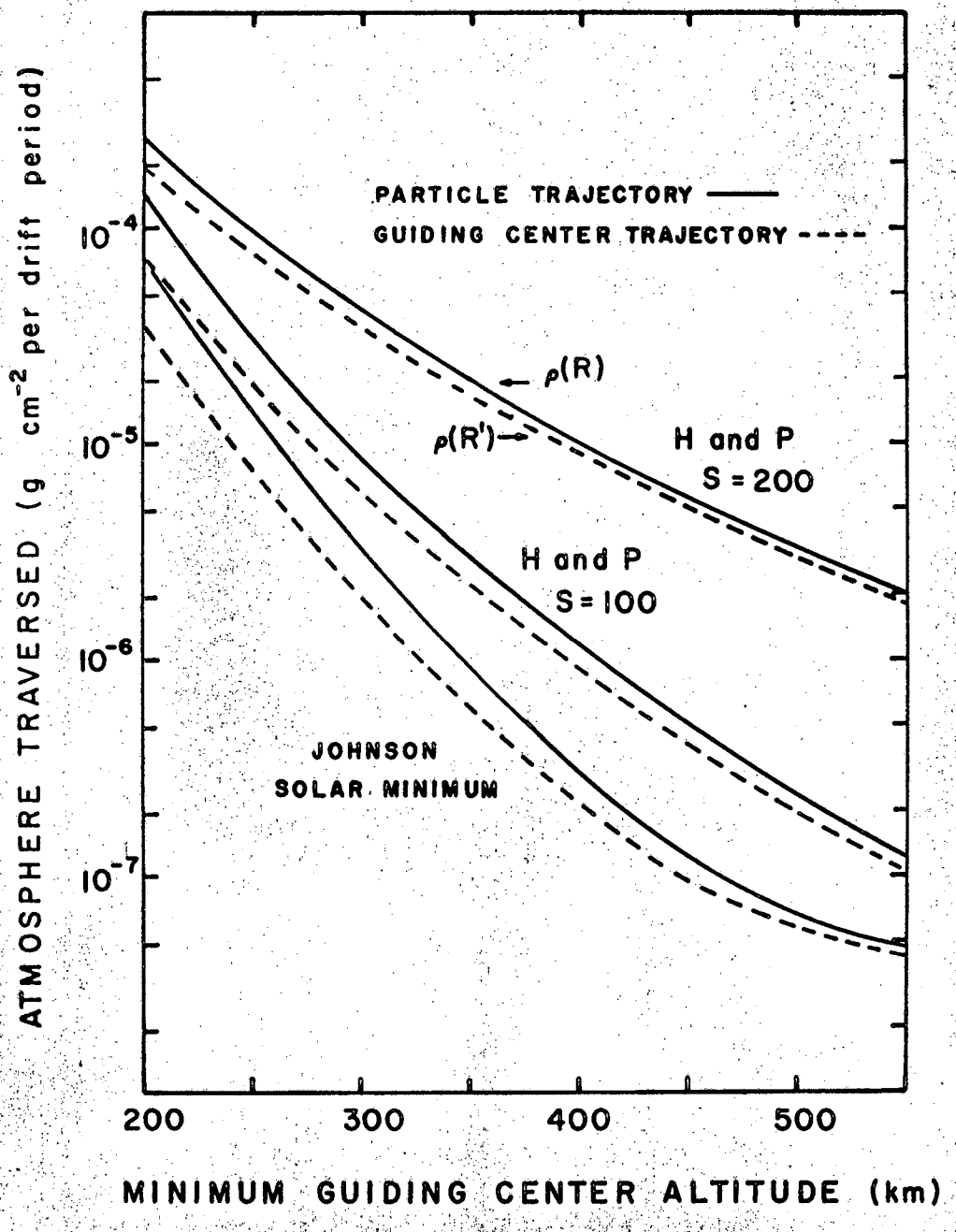

MUB-9096

Fig. 4

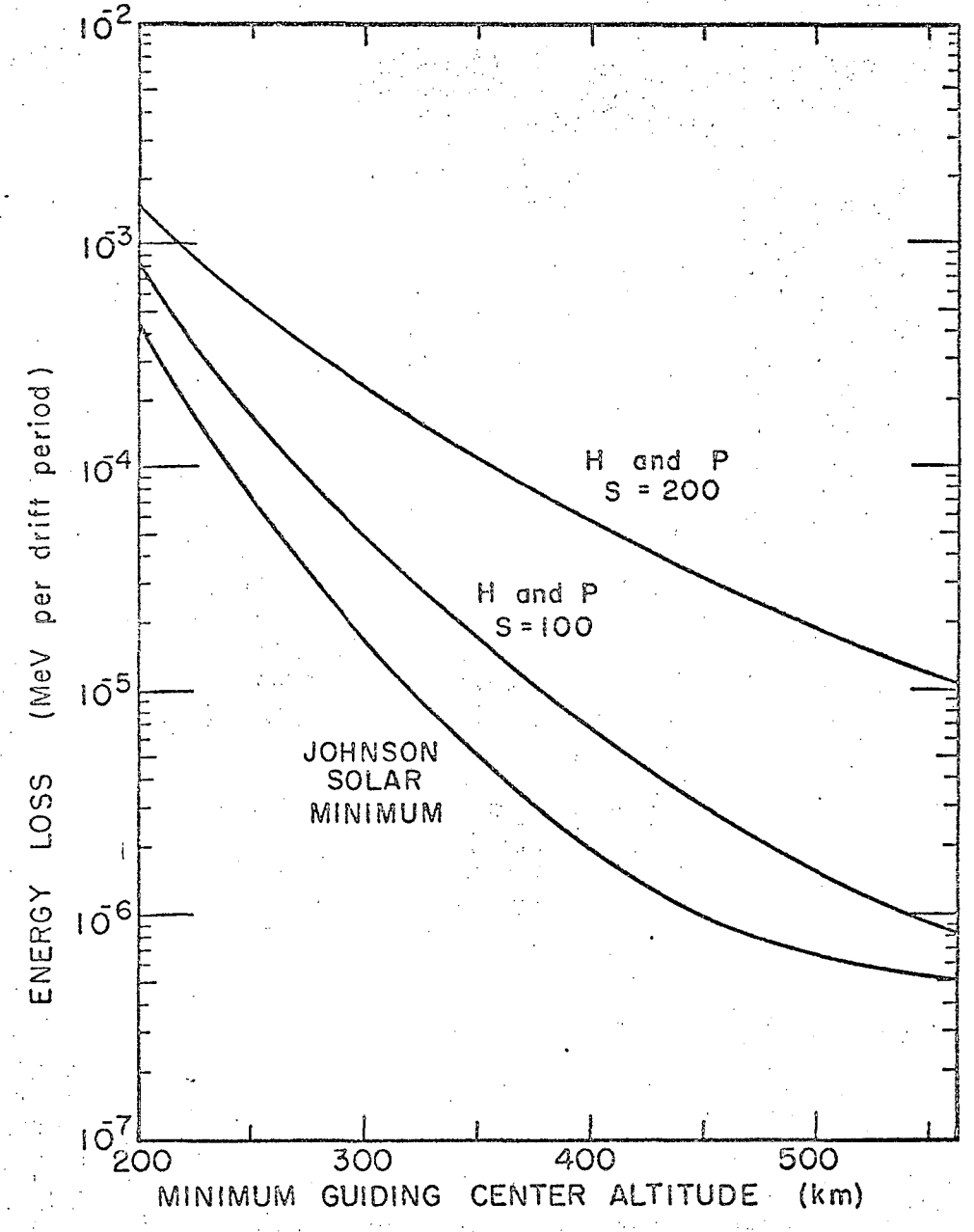
10^{-2}
10^{-3}
10^{-4}
10^{-5}
10^{-6}
10^{-7}
ENERGY LOSS (MeV per drift period)
H and P
S = 200
H and P
S = 100
JOHNSON
SOLAR
MINIMUM
200
300
400
500
MINIMUM GUIDING CENTER ALTITUDE (km)
MUB-9218

Fig. 5

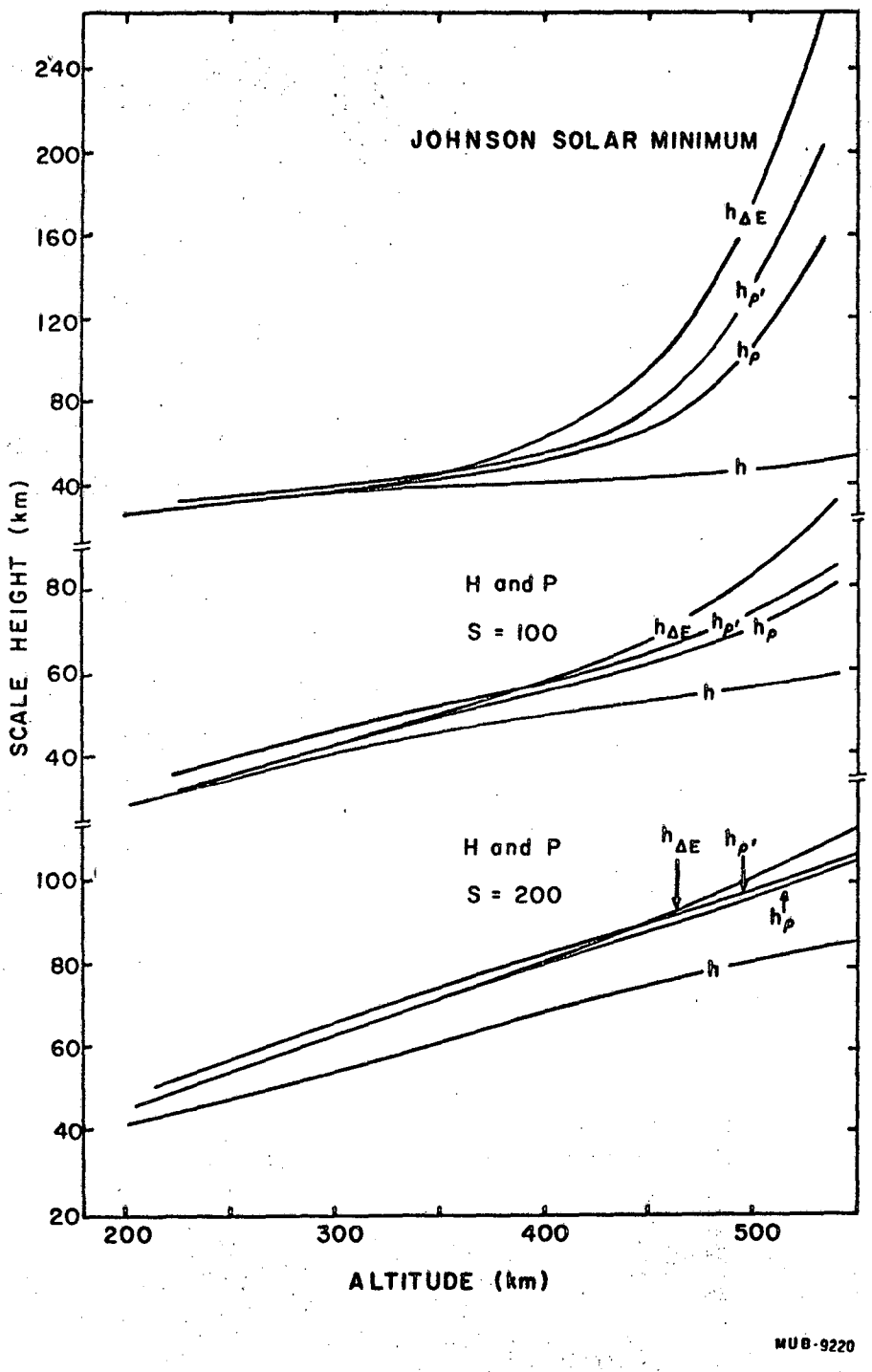
JOHNSON SOLAR MINIMUM
$h_{\Delta E}$
$h_{\rho'}$
h_{ρ}
h
H and P
S = 100
H and P
S = 200
SCALE HEIGHT (km)
ALTITUDE (km)
240
200
160
120
80
40
100
60
20
200
300
400
500
MUB-9220

Fig 6